



# Unitarity Triangle Analysis in the Standard Model and Sensitivity to New Physics\*

M Ciuchini<sup>a</sup>, E Franco<sup>b</sup>, F Parodi<sup>c</sup>, V Lubicz<sup>d,a</sup>, L Silvestrini<sup>b</sup> and A Stocchi<sup>e</sup>

<sup>a</sup>INFN, Sezione di Roma III, Via della Vasca Navale 84, I-00146 Rome, Italy

<sup>b</sup>INFN, Sezione di Roma, P.le Aldo Moro 2, I-00185 Rome, Italy

<sup>c</sup>Dipartimento di Fisica, Università di Genova and INFN, Via Dodecaneso 33, I-16146 Genova, Italy

<sup>d</sup>Dipartimento di Fisica, Università di Roma Tre, Via della Vasca Navale 84, I-00146 Rome, Italy

<sup>e</sup>LAL, IN2P3-CNRS et Université de Paris-Sud, BP 34, F-91898 Orsay Cedex, France

By using the most recent determinations of the several theoretical and experimental input parameters, we update the Unitarity Triangle analysis in the Standard Model and discuss the sensitivity to New Physics effects. We investigate the interest of measuring with a better precision the various physical quantities entering the Unitarity Triangle analysis and study in a model independent way whether, despite the undoubted success of the CKM mechanism in the Standard Model, the Unitarity Triangle analysis still allows the presence of New Physics.

## 1 Introduction

The analysis of the Unitarity Triangle (UT) and CP violation represents one of the most stringent tests of the Standard Model (SM) and, for this reason, also an interesting window on New Physics (NP). The input of this analysis is a large number of both experimental and theoretical parameters, the most relevant of which are listed in Table 1. A careful choice (and a continuous update) of the values of these parameters represents a crucial ingredient in this study, and this was indeed one of the main tasks of the first CKM Workshop. The conclusions of that Workshop have been reported in ref. [1]. In this talk we update the analysis of the UT in the SM by assuming the central values and errors of the input parameters adopted in [1] and collected in Table 1.

The second part of this talk is dedicated to NP. We address two different (though related) questions. The first one concerns the interest of measuring the various physical quantities entering the UT analysis with a better precision. We investigate, in particular, to which extent future and improved determinations of the experimental constraints,  $\sin 2\beta$ ,  $\Delta m_s$  and  $\gamma$ , could allow us to invalidate the SM, thus signalling the presence of NP effects. The second question concerns the possibility of having significant NP contributions in the present analysis of the UT. Given the actual theoretical and experimental constraints, we investigate to which extent the UT analysis can still be affected

\*Talk presented by V. Lubicz

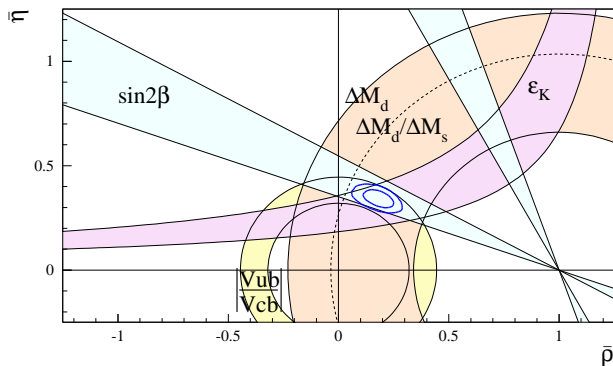


**Figure 1.** Allowed regions for  $\bar{\rho}$  and  $\bar{\eta}$  using the parameters listed in Table 1. The contours at 68% and 95% probability are shown. The full lines correspond to the 95% probability constraints given by the measurements of  $|V_{ub}|/|V_{cb}|$ ,  $|\epsilon_K|$ ,  $\Delta m_d$  and  $\sin 2\beta$ . The dotted curve bounds the region selected at 95% by the lower limit on  $\Delta m_s$ .

by NP contributions. We show that, despite the undoubted success of the SM in describing the flavour sector, large NP contributions in this analysis are in fact still possible (although unnecessary).

## 2 Unitarity Triangle Analysis in the Standard Model

In this section we present the results of the UT analysis assuming the validity of the SM. These results are

Parameter	Value	Gaussian $\sigma$	Theory uncertainty
$\lambda$	0.2240(0.2210)	0.0036 (0.0020)	-
$ V_{cb}  (\times 10^{-3})$ (excl.)	42.1	2.1	-
$ V_{cb}  (\times 10^{-3})$ (incl.)	41.4 (40.4)	0.7	0.6(0.8)
$ V_{ub}  (\times 10^{-4})$ (excl.)	33.0(32.5)	2.4(2.9)	4.6(5.5)
$ V_{ub}  (\times 10^{-4})$ (incl.)	40.9	4.6	3.6
$\Delta M_d$ (ps <sup>-1</sup> )	0.503 (0.494)	0.006 (0.007)	-
$\Delta M_s$ (ps <sup>-1</sup> )	> 14.4 (14.9) at 95% C.L.	sensitivity 19.2 (19.3)	-
$m_t$ (GeV)	167	5	-
$m_c$ (GeV)	1.3	-	0.1
$F_{B_d} \sqrt{\hat{B}_{B_d}}$ (MeV)	223 (230)	33 (30)	12 (15)
$\xi = \frac{F_{B_s} \sqrt{\hat{B}_{B_s}}}{F_{B_d} \sqrt{\hat{B}_{B_d}}}$	1.24(1.18)	0.04 (0.03)	0.06 (0.04)
$\hat{B}_K$	0.86	0.06	0.14
$\sin 2\beta$	0.734 (0.762)	0.054 (0.064)	-

**Table 1.** Values of the relevant quantities used in the fit of the CKM parameters. In the third and fourth columns the Gaussian and the flat parts of the uncertainty are given, respectively. All central values and errors are those adopted in ref. [ 1]. The values within parentheses are the ones available at the time of the first CKM Workshop.

obtained by implementing a Bayesian statistical analysis [ 2] using five independent constraints coming from the determinations of  $|V_{ub}|/|V_{cb}|$ ,  $\Delta m_d$ ,  $\Delta m_s/\Delta m_d$ ,  $\epsilon_K$  and  $\sin 2\beta$ . The regions selected by these constraints in the  $(\bar{\rho}, \bar{\eta})$  plane are shown in Figure 1.

## 2.1 Input parameters

The central values and errors of the input parameters are compared in Table 1 with those available last year at the time of the first CKM Workshop. We discuss here the main variations in central values and/or errors with respect to last year, referring to ref. [ 1] for supporting details.

On the experimental side, the accuracy reached in the determinations of  $\Delta m_d$ ,  $\sin 2\beta$  and also of the  $b \rightarrow u$  semileptonic transitions has further increased. Concerning the  $B_s^0 - \bar{B}_s^0$  oscillations, the likelihood now prefers slightly smaller values of  $\Delta m_s$ , so that the lower limit on this quantity is slightly decreased while the sensitivity remains almost unchanged. In addition, a more critical look at the experimental results leading to the determination of the Cabibbo angle  $\lambda$  has produced a significant increase on both the central value and the uncertainty assigned to this quantity [ 1], the latter being increased by approximately 80% with respect to last year. Since, however,  $\lambda$  is known with a very good relative accuracy, these changes have a marginal impact on the results of the UT analysis.

On the theoretical side, a significant improvement concerns the uncertainty on the inclusive determination of  $|V_{cb}|$  which is reduced, at present, to the impressive level of 1%. Another important change, which is

worth mentioning, concerns the theoretical estimate of the so called ‘‘chiral logs effects’’ in the lattice evaluation of  $F_{B_d} \sqrt{\hat{B}_{B_d}}$ , which is mostly reflected in the final estimate of  $\xi$  (see Table 1). For this ratio, the central value has increased by approximately 5% but the corresponding relative uncertainty has been estimated to increase by almost 50%. Since the estimate of this uncertainty is not based directly on lattice data, one can reasonably expect that it will be reduced in a rather short time [ 3].

## 2.2 The apex of the UT: $\bar{\rho}$ and $\bar{\eta}$

By using all five constraints ( $|V_{ub}|/|V_{cb}|$ ,  $\Delta m_d$ ,  $\Delta m_s/\Delta m_d$ ,  $\epsilon_K$  and  $\sin 2\beta$ ), the following results for  $\bar{\rho}$  and  $\bar{\eta}$  are obtained

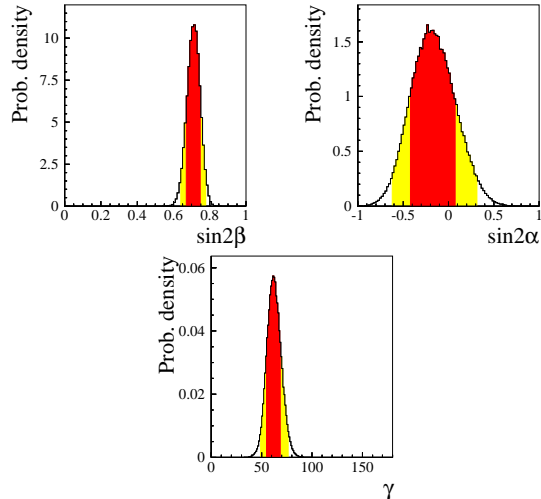
$$\begin{aligned} \bar{\rho} &= 0.178 \pm 0.046 & [0.085 - 0.265] \text{ at 95\% C.L.} \\ \bar{\eta} &= 0.341 \pm 0.028 & [0.288 - 0.397] \text{ at 95\% C.L.} \end{aligned} \quad (1)$$

Figure 1 shows the region in the  $(\bar{\rho}, \bar{\eta})$  plane selected by the contours at 68% and 95% probability.

## 2.3 The angles: $\sin 2\beta$ , $\sin 2\alpha$ and $\gamma$ .

The p.d.f. obtained for  $\sin 2\beta$ ,  $\sin 2\alpha$  and  $\gamma$  are shown in Figure 2.

It is useful to recall that one of the most important results of the UT analysis was the prediction of  $\sin 2\beta$ . The value of  $\sin 2\beta$  was determined, well before its first direct measurement, by using all the other available constraints, namely  $|V_{ub}|/|V_{cb}|$ ,  $|\epsilon_K|$ ,  $\Delta m_d$  and  $\Delta m_s$ .



**Figure 2.** The p.d.f. for  $\sin 2\beta$ ,  $\sin 2\alpha$  and  $\gamma$ .

The accuracy of these predictions was rather good. For instance, at the end of 2000 the following indirect determination was obtained [ 2]

$$\sin 2\beta = 0.698 \pm 0.066 \quad \text{all constraints but } A_{CP} \quad (2)$$

to be compared with the present direct measurement

$$\sin 2\beta = 0.734 \pm 0.054 \quad A_{CP}(J/\psi K_s). \quad (3)$$

The indirect determination obtained today, by using the values of the input parameters collected in Table 1, is

$$\sin 2\beta = 0.685 \pm 0.052 \quad \text{all constraints but } A_{CP} \quad (4)$$

It can be noticed that the present precision for the direct and the indirect measurements are similar. When combined, one obtains the best estimate

$$\sin 2\beta = 0.705^{+0.042}_{-0.032} \quad [0.636 - 0.779] \text{ at 95\% C.L.} \quad (5)$$

The p.d.f. of  $\sin 2\alpha$ , presented in Figure 2, shows that the angle  $\alpha$  is much less constrained by the UT analysis than the angle  $\beta$ . This distribution corresponds to the result

$$\sin 2\alpha = -0.19 \pm 0.25 \quad [-0.62 - 0.33] \text{ at 95\% C.L.} \quad (6)$$

The angle  $\gamma$  is predicted with an accuracy which is at present of about 10%:

$$\gamma = (61.5 \pm 7.0)^\circ \quad [49.0 - 77.0]^\circ \text{ at 95\% C.L.} \quad (7)$$

The effects of chiral logs in the lattice evaluation of  $\xi$  are included in this determination, although the change in  $\gamma$  is not significant (the previous value was  $59.5^{+6.5}_{-5.5}$  [ 4]). It should also be stressed that, with present measurements, the probability that  $\gamma$  is greater than  $90^\circ$  is only 0.003.

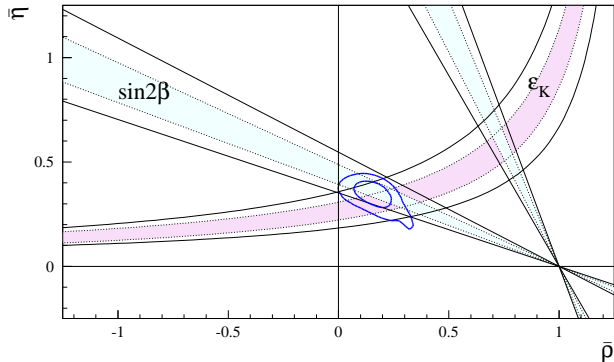


**Figure 3.** The allowed regions for  $\bar{\rho}$  and  $\bar{\eta}$  (contours at 68%, 95%) as selected by the measurements of  $|V_{ub}|/|V_{cb}|$ ,  $\Delta M_d$ , and by the limit on  $\Delta M_s/\Delta M_d$  are compared with the bands (at 68% and 95% C.L.) from the measurements of CP violating quantities in the kaon ( $\epsilon_K$ ) and in the B ( $\sin 2\beta$ ) sectors.

## 2.4 Indirect evidence of CP violation

An important test of the SM in the UT analysis is the comparison between the region selected by the measurements which are sensitive only to the sides of the UT (CP conserving semileptonic B decays and  $B^0 - \bar{B}^0$  oscillations) and the regions selected by the direct measurements of CP violation in the kaon ( $\epsilon_K$ ) and in the B ( $\sin 2\beta$ ) sectors. This test is shown in Figure 3.

The result can be made quantitative by comparing the values of  $\sin 2\beta$  obtained from the measurement of the CP asymmetry in the  $J/\psi K_s$  decays with those determined from “sides” measurements only:

$$\begin{aligned} \sin 2\beta &= 0.695 \pm 0.056 \quad \text{Sides only} \\ \sin 2\beta &= 0.734 \pm 0.054 \quad A_{CP}(J/\psi K_s). \end{aligned} \quad (8)$$

The spectacular agreement between these results illustrates the consistency of the SM in describing the CP violation phenomena through the CKM mechanism, in terms of a single parameter  $\eta$ . Moreover, it provides an important test of the calculations based on the OPE, the HQET and the lattice QCD approaches which have been used to extract the CKM parameters.

## 2.5 Determination of $\Delta m_s$

Another important result of the UT analysis is the possibility to extract the probability distribution for the mass difference  $\Delta m_s$ , which is shown in Figure 4. The corresponding results, obtained either by using or not using the experimental information coming from the analysis of the  $B_s^0 - \bar{B}_s^0$  oscillations, are

$$\Delta m_s = 18.3^{+1.7}_{-1.5} \quad [15.6 - 22.2] \text{ at 95\% C.L.}$$

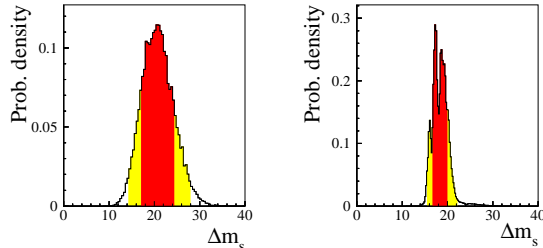


**Figure 4.**  $\Delta m_s$  probability distributions. The information from  $B_s^0 - \bar{B}_s^0$  oscillations is used (not used) in the right (left).

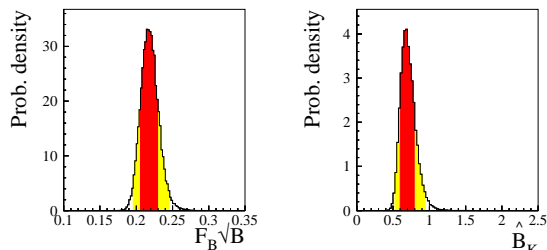


**Figure 5.** The p.d.f. for  $F_{B_d}\sqrt{\hat{B}_{B_d}}$  (left) and  $B_K$  (right).

$$\Delta m_s = 20.6 \pm 3.5 \quad [14.2 - 28.1] \text{ at 95\% C.L.} \quad (9)$$

with  $\Delta m_s$   
without  $\Delta m_s$

The present limit (from LEP and SLD) excludes already a fraction of the  $\Delta m_s$  distribution. Present analyses at LEP/SLD are situated in a high probability region for a positive signal (as the “signal bump” appearing around  $17 \text{ ps}^{-1}$ ). Accurate measurements of  $\Delta m_s$  are expected soon from the TeVatron. The result in the second of Equations (9) represents another significant prediction of the UT analysis.

## 2.6 Determination of $F_{B_d}\sqrt{\hat{B}_{B_d}}$ and $B_K$

Since the UT fits in the SM are currently overconstrained, they can also be used to extract a determination of one (or some) of the relevant hadronic parameters entering the analysis. This determination then provides a useful comparison for the corresponding theoretical predictions obtained from lattice QCD simulations.

The p.d.f. of  $F_{B_d}\sqrt{\hat{B}_{B_d}}$  is shown in Figure 5 (left). From this distribution one obtains

$$F_{B_d}\sqrt{\hat{B}_{B_d}} = (217 \pm 12) \text{ MeV} \quad (10)$$

which is in very good agreement with the lattice determination given in Table 1. Notice also that  $F_{B_d}\sqrt{\hat{B}_{B_d}}$

is determined with an accuracy which is better than the current evaluation from lattice QCD.

The density distribution for the parameter  $B_K$  is given in Figure 5 (right). The fitted value is

$$B_K = 0.69^{+0.11}_{-0.09}, \quad (11)$$

which is in agreement, though one standard deviation smaller, with the corresponding lattice estimate. By looking at the uncertainty obtained in Equation (11) one concludes that the present estimate of  $B_K$  from lattice QCD, with a 15% relative error, has a large impact in the present analysis.

Notice that values of  $B_K$  smaller than 0.5 (0.3) have a probability of 0.6% ( $5 \times 10^{-6}$ ), whereas values of  $B_K$  larger than 1.0 have a probability of 1.3%. In disfavoring large values of  $B_K$  the direct measurement of  $\sin 2\beta$  plays a crucial role.

The results above on either  $F_{B_d}\sqrt{\hat{B}_{B_d}}$  or  $\hat{B}_K$  are obtained by using the theoretical information coming from the distributions of both the other parameter and  $\xi$ . It is interesting to see if significant results can be obtained by removing simultaneously two of the previous constraints.

The region in the plane  $(F_{B_d}\sqrt{\hat{B}_{B_d}}, \hat{B}_K)$ , which is obtained by removing the theoretical constraints on these quantities, is shown in Figure 6 (top). Within 68% and 95% probabilities, both  $F_{B_d}\sqrt{\hat{B}_{B_d}}$  and  $\hat{B}_K$  are well constrained. The most important conclusion which can be drawn from this study is the simultaneous range obtained for  $F_{B_d}\sqrt{\hat{B}_{B_d}}$  and  $\hat{B}_K$ , namely

$$\hat{B}_K = 0.69^{+0.13}_{-0.08} \quad [0.53 - 0.96] \quad (12)$$

$$F_{B_d}\sqrt{\hat{B}_{B_d}} = 203^{+17}_{-13} \text{ MeV} \quad [180 - 242] \text{ MeV}$$

The same analysis can be performed by removing also the information coming from  $\Delta m_s$ , namely removing the external constraint controlled by the non perturbative QCD parameter  $\xi$ . The region obtained in the plane  $(F_{B_d}\sqrt{\hat{B}_{B_d}}, \hat{B}_K)$  is shown in Figure 6 (bottom) and corresponds to

$$\hat{B}_K = 0.67^{+0.26}_{-0.13} \quad [0.47 - 1.27] \quad (13)$$

$$F_{B_d}\sqrt{\hat{B}_{B_d}} = 203^{+38}_{-28} \text{ MeV} \quad [162 - 278] \text{ MeV}$$

This last result relies only on the  $|V_{ub}|/|V_{cb}|$  and  $\sin 2\beta$  constraints, and it is thus only dependent on the hadronic parameters entering the  $B$  semileptonic decays.

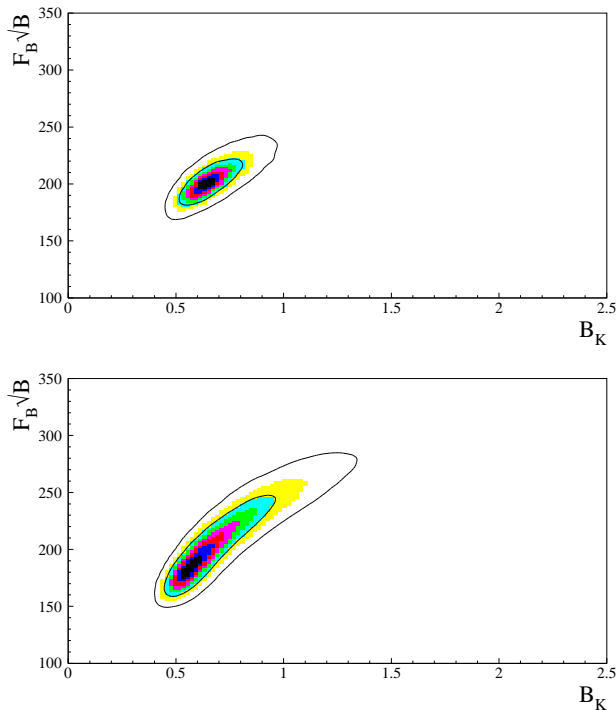


**Figure 6.** The 68% and 95% contours in the  $(F_{B_d}\sqrt{\hat{B}_{B_d}}, \hat{B}_K)$  plane. The plot on the top is obtained using the  $|V_{ub}|/|V_{cb}|$ ,  $\Delta m_s$  and  $\sin 2\beta$  constraints, while in the bottom one also the information from  $\Delta m_s$  (and thus  $\xi$ ) has been removed.

### 3 New Physics: impact of future (and more precise) measurements

In this section we would like to discuss the interest of measuring the various physical quantities entering the UT analysis with a better precision. We investigate, in particular, to which extent future and improved determinations of the experimental constraints,  $\sin 2\beta$ ,  $\Delta m_s$  and  $\gamma$ , could allow us to possibly invalidate the SM, thus signalling the presence of NP effects.

#### 3.1 $\sin 2\beta$

We start this analysis by considering the measurement of  $\sin 2\beta$ . The plot in Figure 7 shows the compatibility (“pull”) between the direct and indirect distributions of  $\sin 2\beta$ , in the SM, as a function of the (hypothetical) measured value of  $\sin 2\beta$ , parametrized for different values of the errors. The compatibility between the two distributions is determined by using the p.d.f. of the difference between the direct and the indirect determinations. The compatibility is then evaluated by mean of the ratio between the central value of this resulting (pseudo-Gaussian) distribution and its standard deviation.

From the plot in Figure 7 it can be seen that, consid-

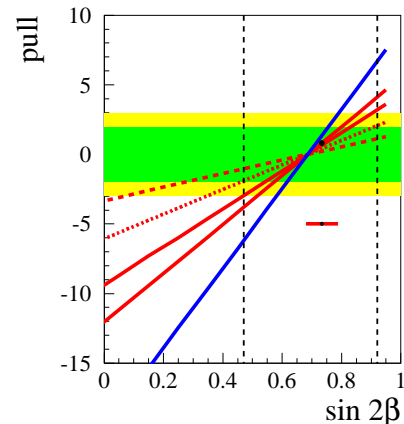


**Figure 7.** The compatibility (“pull”) between the direct and indirect determination of  $\sin 2\beta$  as a function of the value of  $\sin 2\beta$  measured from CP asymmetry in  $J/\psi K_s$  decays. The different curves correspond to different errors for  $\sin 2\beta$  (from top to bottom 0.2, 0.1, 0.05 and 0.02). The last curve (darker) corresponds to the scenario in which all the experimental and theoretical errors contributing to the indirect measurement of  $\sin 2\beta$  are reduced by a factor of two. The point indicate the situation for the present measurement. The horizontal bands indicate the 2 and 3  $\sigma$  compatibility regions. The 3 $\sigma$  region which corresponds to an error of 0.05 on  $\sin 2\beta$  is indicated by the vertical dotted lines.

ering the actual precision of about 0.05 on the measured value of  $\sin 2\beta$ , the 3 $\sigma$  compatibility region is between [0.46-0.92]. Values outside this range would be, therefore, not compatible with the SM prediction at more than 3 $\sigma$  level. To get these values, however, the presently measured central value should shift by more than 4 $\sigma$ .

Figure 7 also shows that, in case the experimental error on  $\sin 2\beta$  was 0.02, the compatibility region would be reduced to [0.52-0.86]. Furthermore, if all the errors contributing to the indirect determination of  $\sin 2\beta$  are decreased by a factor of two that region is reduced by more than a factor 1.5 (as shown by the darker curve).

The conclusion that can be derived from Figure 7 is the following: although the improvement of the error  $\sin 2\beta$  has an important impact on the accuracy of the UT parameter determination, it is very unlikely that in the near future we will be able to use this measurement to detect any failure of the SM, unless the central value of the direct measurement will move away from the present one by several standard deviations.

It was pointed out sometime ago that the comparison of the time dependent CP asymmetries in various  $B$ -decay modes could provide evidence of NP [5]. Beside the  $J/\psi K_s$  mode, the asymmetry  $A_{CP}(\phi K_s)$  also allows to extract  $\sin 2\beta$  with negligible hadronic uncertainties [6]. Furthermore the  $\phi K_s$  mode is expected to

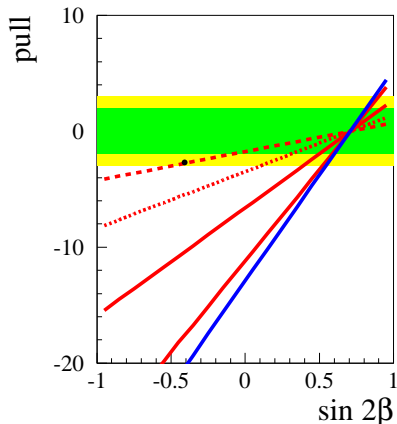


**Figure 8.** The compatibility of the direct and indirect determination of  $\sin 2\beta$  as a function of the value of  $\sin 2\beta$  measured from CP asymmetry in  $\phi K_s$  decays. The different curves correspond to different errors for  $\sin 2\beta$  (from top to bottom 0.4, 0.2, 0.1 and 0.05). The point indicate the situation for the present measurement. The last curve (darker) corresponds to the scenario in which all the experimental and theoretical errors contributing to the indirect measurement of  $\sin 2\beta$  are reduced by a factor of two. The horizontal bands indicate the 2 and 3  $\sigma$  compatibility regions.

be more sensitive to NP being a pure penguin process.

This asymmetry has been recently measured at the B-factories [ 7]:

$$\sin 2\beta = -0.39 \pm 0.41 \quad \phi K_s \text{ mode} \quad (14)$$

The plot in Figure 8 shows the compatibility of the direct and indirect distributions of  $\sin 2\beta$  as a function of the measured value of  $\sin 2\beta$  parametrized for different errors. The difference with respect to the plot in Figure 7 is that in this case all the available constraints have been used to obtain the indirect distribution of  $\sin 2\beta$ , including the direct measurement of  $\sin 2\beta$  from  $J/\psi K_s$ .

It can be noticed that the current measured value in the  $\phi K_s$  mode is at  $2.7\sigma$  deviation from the expected one. This deviation is obviously dominated by the experimental error on the measured CP asymmetry, and its significance is not really affected if some or even all the theoretical errors are multiplied by a factor of two. Keeping the same central value a reduction of a factor of two in the experimental error will shift the significance to  $5.7\sigma$  and any measured value below zero will deviate by more than  $4\sigma$  from the SM prediction.

### 3.2 $\Delta m_s$

The plot in Figure 9 shows the compatibility of the indirect determination of  $\Delta m_s$  with a future determination of the same quantity. It can be noted that the

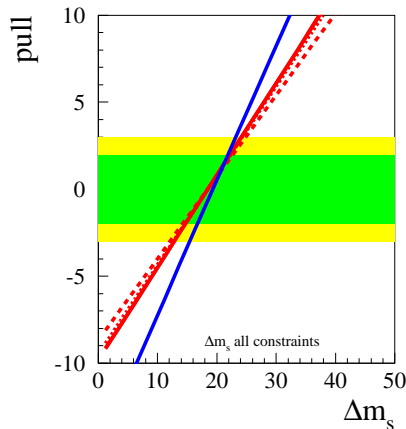


**Figure 9.** Same as in Figure 8 but for  $\Delta m_s$ . The different curves correspond to different errors for this determination (from bottom to top 1, 0.5, 0.2 and 0.1  $\text{ps}^{-1}$ ).

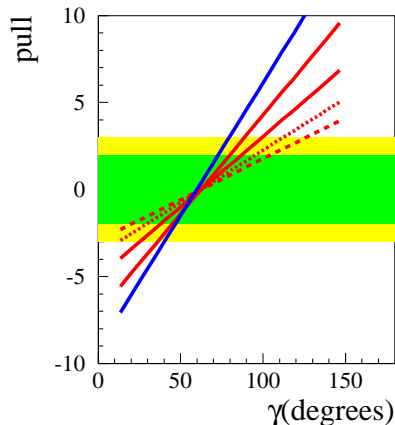


**Figure 10.** Same as in Figure 8 but for  $\gamma$ . The different curves correspond to different errors for this determination (from bottom to top 20, 15, 10 and 5 degrees).

predicted ranges for  $\Delta m_s$  which are compatible within  $3\sigma$  with the SM prediction do not really depend on the accuracy of the future measurement. Furthermore these ranges will be not much affected by a reduction of the errors of the quantities entering in the indirect determination. From the plot in Figure 9 it can be concluded that

$$\begin{aligned} \Delta m_s &> 29 \text{ (28) [26] } \text{ps}^{-1} && \text{“New Physics” at } 5 \sigma \text{ (15)} \\ \Delta m_s &> 25 \text{ (24) [23] } \text{ps}^{-1} && \text{“New Physics” at } 3 \sigma \end{aligned}$$

corresponding to 1  $\text{ps}^{-1}$  (0.1  $\text{ps}^{-1}$ ) [0.1  $\text{ps}^{-1}$  with all the errors divided by two] scenarios.

### 3.3 The angle $\gamma$

The angle  $\gamma$  can be also extracted, in principle, from the measurements of two-body charmless hadronic B

Tree-Level	$B_d^0$ mixing (1,3) family	$B_s^0$ mixing (2,3) family	$K^0$ mixing (1,2) family
$ V_{ub} / V_{cb} $	$\Delta m_d$ and $A_{CP}(J/\Psi\phi)$	$\Delta m_s$	$\epsilon_K$

**Table 2.** *Different processes and corresponding measurements contributing to the determination of  $\bar{\rho}$  and  $\bar{\eta}$ .*

decays. A lot of theoretical investigations have been recently made for these decay channels. In particular, important progress has been made with the calculation of the amplitudes in the heavy quark limit using the factorization approach [ 8], though there is still some controversy on the importance of non-leading corrections [ 9].

From the experimental point of view an impressive effort has been made to measure as many branching fractions and CP asymmetries as possible (for a collection of results see [ 10]). It would be very interesting in the near future to compare the determination of the angle  $\gamma$  from the UT analysis and from two-body decays measurements. In the future, at the LHC/BTeV experiments,  $\gamma$  will be cleanly measured in the tree-level  $B_s \rightarrow DK$  decays.

The plot in Figure 10 shows the compatibility of the indirect determination of  $\gamma$  with a future determination of the same angle obtained from B decays. It can be noted that even in case the angle  $\gamma$  can be measured with a precision of  $10^\circ$  from B decays, the predicted  $3\sigma$  region is still rather large, corresponding to the interval  $[25-100]^\circ$ . If all the theoretical errors are divided by a factor of two, as indicated by the darker curve, the predicted  $3\sigma$  region will be consistently reduced.

## 4 New Physics: a (simplified) Model Independent analysis

Although the CKM mechanism is extremely successful, leading in particular to the precise prediction of the value of  $\sin 2\beta$ , it is nevertheless worth to investigate whether the analysis of the UT still allows some room for NP effects. This is the issue we would like to address in this section.

The physical processes entering the analysis and the related physical observables determined from the experiments, are listed in Table 2. Barring the possibility of significant NP effects in the determination of the ratio  $|V_{ub}|/|V_{cb}|$  from tree-level processes, we have explored the possible contributions to  $B_q^0 - \bar{B}_q^0$  mixing ( $q = d, s$ ) and  $K^0 - \bar{K}^0$  mixing.

NP contributions introduce in general a large number of new parameters: flavour changing couplings, short distance coefficients and matrix elements of new local operators. The specific list and the actual values of these parameters depend on the details of the NP

model. Nevertheless, each of the mixing process listed in Table 2, being described by a single amplitude, can be effectively parameterized in a completely general way in terms of only two new parameters, which we choose to quantify the difference of the amplitude in absolute value and phase with respect to the SM one [ 11]. Thus, for instance, in the case of  $B_q^0 - \bar{B}_q^0$  mixings we define

$$C_q e^{2i\phi_q} = \frac{\langle B_q^0 | H_{eff}^{full} | \bar{B}_q^0 \rangle}{\langle B_q^0 | H_{eff}^{SM} | \bar{B}_q^0 \rangle} \quad (q = d, s) \quad (16)$$

where  $H_{eff}^{SM}$  includes only the SM box diagrams, while  $H_{eff}^{full}$  includes also the NP contributions. By definition, in the absence of NP effects,  $C_q = 1$  and  $\phi_q = 0$ . The experimental quantities determined from the  $B_q^0 - \bar{B}_q^0$  mixings and listed in Table 2 are related to their SM counterparts and the NP parameters by the following relations:

$$\begin{aligned} \Delta m_d &= C_d \Delta m_d^{SM} & (B_d^0 - \bar{B}_d^0 \text{ mixing}) \\ A_{CP}(J/\Psi K_s) &= \sin 2(\beta + \phi_d) \end{aligned} \quad (17)$$

and

$$\Delta m_s = C_s \Delta m_s^{SM} \quad (B_s^0 - \bar{B}_s^0 \text{ mixing}). \quad (18)$$

As far as the  $K^0 - \bar{K}^0$  mixing is concerned, we find it convenient to introduce a single parameter which relates the imaginary part of the amplitude to the SM one

$$C_\epsilon = \frac{\text{Im}[\langle K^0 | H_{eff}^{full} | \bar{K}^0 \rangle]}{\text{Im}[\langle K^0 | H_{eff}^{SM} | \bar{K}^0 \rangle]}. \quad (19)$$

This definition implies in fact a simple relation for  $|\epsilon_K|$ ,

$$|\epsilon_K| = C_\epsilon |\epsilon_K|^{SM} \quad (K^0 - \bar{K}^0 \text{ mixing}) \quad (20)$$

Thus, all NP effects which may enter the present analysis of the UT are parameterized in terms of four real coefficients,  $C_d$ ,  $\phi_d$ ,  $C_s$  and  $C_\epsilon$ .

Due to the limited available number of constraints, we now make the hypothesis that NP effects can appear (at least to a large extent) only in one of the three mixing amplitudes. This is the only restrictive assumption

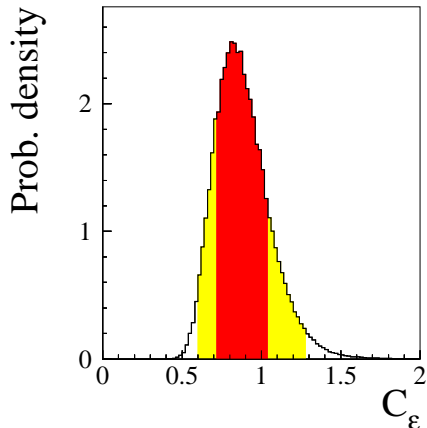


**Figure 11.** The  $C_\epsilon$  distribution obtained by leaving this parameter free in the fit and assuming the SM parameterization for  $|V_{ub}|/|V_{cb}|$ ,  $\Delta m_d$ ,  $\Delta m_s/\Delta m_d$  and  $\sin 2\beta$ .

we make in this analysis. Clearly, this hypothesis is not valid in several specific models, as for instance in the Minimal Flavour Violating SUSY models [12] in which NP effects simultaneously appear in all the mixing amplitudes but with coefficients which are related one to the other.

We start the analysis by considering NP contributions in  $K^0 - \bar{K}^0$  mixing. Figure 11 shows the distribution of the parameter  $C_\epsilon$ . The result from the fit is:

$$C_\epsilon = 0.85^{+0.20}_{-0.14} \quad [0.60 - 1.28] \text{ at 95\% C.L.} \quad (21)$$

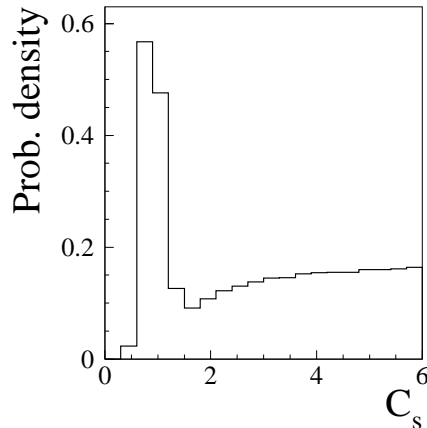
The value is compatible with unity but the distribution is rather broad. Thus, in this respect, large NP contributions to  $K^0 - \bar{K}^0$  mixing are still allowed. We note, however, that the experimental constraint coming from  $|\varepsilon_K|$  can only determine the product  $C_\epsilon \cdot B_K$ . Therefore, the large width of the distribution of  $C_\epsilon$  simply reflects the uncertainty existing on the hadronic parameter  $B_K$ . We also find that, in this scenario, the distributions of the other UT parameters ( $\bar{\rho}$ ,  $\bar{\eta}$ ,  $\sin 2\beta$ , ...) are not really different from those obtained using the SM parameterization ( $C_\epsilon = 1$ ).

Figure 12 shows the distribution of the parameter  $C_s$  entering the  $B_s^0 - \bar{B}_s^0$  mixing amplitude.

The value of  $C_s$  peaks at 1. However, it is not limited from above due to the fact the  $\Delta m_s$  is not yet determined. Also in this case, the distributions of the other UT parameters are not really different from those obtained using the SM parameterization ( $C_s = 1$ ).

Finally we explore the possibility of NP contributions in  $B_d^0 - \bar{B}_d^0$  mixing. Figure 13 shows the distributions of  $C_d$  and  $\phi_d$ .<sup>2</sup>

<sup>2</sup>The angle  $\phi_d$  is determined from the measurement of  $A_{CP}(J/\psi K_s)$  up to a discrete ambiguity,  $\phi_d + \beta \rightarrow \pi - \phi_d - \beta$ . In Figure 13 only one of the two determinations (the one containing  $\phi_d = 0$ ) is shown for clarity.



**Figure 12.** The  $C_s$  distribution obtained by leaving this parameter free in the fit and assuming the SM parameterization for  $|V_{ub}|/|V_{cb}|$ ,  $\Delta m_d$ ,  $|\varepsilon_K|$  and  $\sin 2\beta$ .

We see that two solutions are possible in this case. The first one peaks around the SM solution,  $C_d \simeq 1$  and  $\phi_d \simeq 0$ . The second one represents instead the possibility of a really distinct NP contribution. The presence of two solutions corresponds to the fact that, as shown in Figure 14, the constraint from  $|\varepsilon_K|$  intercepts the circle defined by  $|V_{ub}|/|V_{cb}|$  in two regions. The region on the quadrant with positive value of  $\bar{\rho}$  corresponds to the SM solution. The presence of these two solutions is also visible in several distributions of the UT parameters shown in Figure 15. As can be seen from these plots, in order to discriminate between the two solutions, an independent determination of either  $\bar{\rho}$ , as obtained for instance from the study of the ratio  $\Gamma(B \rightarrow K^* \gamma)/\Gamma(B \rightarrow \rho \gamma)$  of radiative  $B$  decays, or  $\gamma$  would be necessary. The NP solution has been also recently discussed in the literature [13].

We want to conclude this discussion with a comment concerning the “naturalness” of this “NP solution”. First, we observe that NP, though possible, is certainly not required in order to explain the results of the UT analysis. In addition, suppose that the NP solution in  $B_d^0 - \bar{B}_d^0$  mixing is indeed the correct one. Then it is somewhat surprising to find that in the SM, i.e. in the “wrong” theory of  $B_d^0 - \bar{B}_d^0$  mixing, the predicted values of  $\Delta m_d$  and  $\sin 2\beta$  actually select in the  $(\bar{\rho}, \bar{\eta})$  plane just one of the two regions which are also allowed by the other constraints, namely  $|V_{ub}|/|V_{cb}|$  and  $|\varepsilon_K|$ . In this sense, the consistency of this NP solution would be accidental.

## References

1. M. Battaglia *et al.*, arXiv:hep-ph/0304132.
2. M. Ciuchini *et al.*, JHEP **0107** (2001) 013 [arXiv:hep-ph/0012308].
3. D. Becirevic, talk presented at This Workshop.



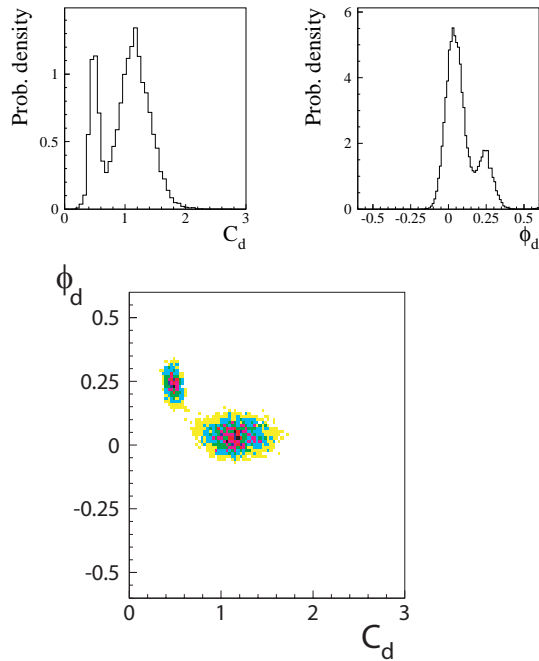


**Figure 13.** The  $C_d$  and  $\phi_d$  distributions obtained by leaving these parameters free in the fit and the SM parameterization for  $|V_{ub}|/|V_{cb}|$  and  $|\varepsilon_K|$  and  $\Delta m_s$ .

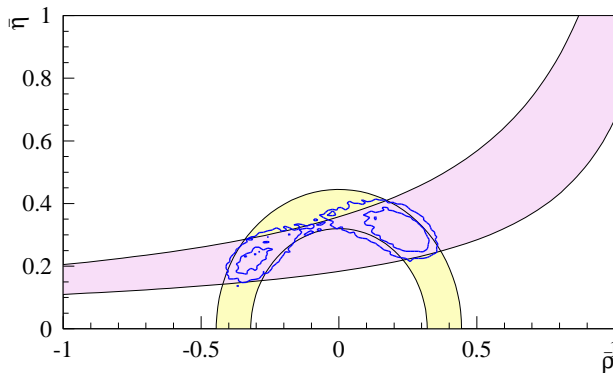


**Figure 14.** The allowed regions for  $\bar{\rho}$  and  $\bar{\eta}$  (contours at 68% and 95%) as selected the measurements of  $|V_{ub}|/|V_{cb}|$  and  $|\varepsilon_K|$ . The bands at 95% C.L. from the two constraints are also shown.

4. F. Parodi, talk at ICHEP02 (26-31/7/2002 Amsterdam)
5. Y. Grossman and M. P. Worah, Phys. Lett. B **395** (1997) 241 [arXiv:hep-ph/9612269].  
M. Ciuchini *et al.*, Phys. Rev. Lett. **79** (1997) 978 [arXiv:hep-ph/9704274].
6. D. London and A. Soni, Phys. Lett. B **407** (1997) 61 [arXiv:hep-ph/9704277].  
Y. Grossman, G. Isidori and M. P. Worah, Phys. Rev. D **58** (1998) 057504 [arXiv:hep-ph/9708305].
7. B. Aubert *et al.* [BABAR Collaboration],

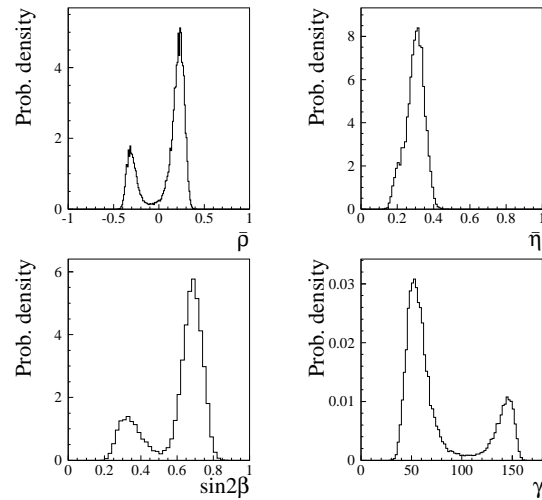


**Figure 15.** The p.d.f. for  $\bar{\rho}$ ,  $\bar{\eta}$ ,  $\sin(2\beta)$  and  $\gamma$  obtained when the NP parameters  $C_d$  and  $\phi_d$  are left free in the fit and the SM parameterization for  $|V_{ub}|/|V_{cb}|$  and  $|\varepsilon_K|$  are used.

arXiv:hep-ex/0207070.

K. Abe *et al.* [Belle Collaboration],

arXiv:hep-ex/0207098.

8. M. Beneke, G. Buchalla, M. Neubert and C. T. Sachrajda, Phys. Rev. Lett. **83** (1999) 1914 [arXiv:hep-ph/9905312]; Nucl. Phys. B **591** (2000) 313 [arXiv:hep-ph/0006124]; Nucl. Phys. B **606** (2001) 245 [arXiv:hep-ph/0104110].
9. M. Ciuchini *et al.*, AIP Conf. Proc. **602** (2001) 180 [arXiv:hep-ph/0110022]; Phys. Lett. B **515** (2001) 33 [arXiv:hep-ph/0104126].
10. A. Stocchi, Nucl. Phys. Proc. Suppl. **117** (2003) 145 [arXiv:hep-ph/0211245].
11. J. M. Soares and L. Wolfenstein, Phys. Rev. D **47** (1993) 1021.  
N. G. Deshpande, B. Dutta and S. Oh, Phys. Rev. Lett. **77** (1996) 4499 [arXiv:hep-ph/9608231].  
J. P. Silva and L. Wolfenstein, Phys. Rev. D **55** (1997) 5331 [arXiv:hep-ph/9610208].  
A. G. Cohen *et al.*, Phys. Rev. Lett. **78** (1997) 2300 [arXiv:hep-ph/9610252].  
Y. Grossman, Y. Nir and M. P. Worah, Phys. Lett. B **407** (1997) 307 [arXiv:hep-ph/9704287].
12. M. Ciuchini *et al.*, Nucl. Phys. B **534** (1998) 3 [arXiv:hep-ph/9806308].  
A. J. Buras *et al.*, Phys. Lett. B **500** (2001) 161 [arXiv:hep-ph/0007085].
13. R. Fleischer, G. Isidori and J. Matias, JHEP **0305** (2003) 053 [arXiv:hep-ph/0302229].  
G. Isidori, arXiv:hep-ph/0307014.